Structure and Mechanical Properties of Chitosan/Poly(Vinyl Alcohol) Blend Films

Yumiko Nakano,[1] *Yuezhen Bin,*[1] *Mami Bando,*[1] *Teruo Nakashima,*[2] *Tsumuko Okuno,*[3] *Hiromichi Kurosu,*[1] *Masaru Matsuo**[1]

Summary: The origins of the thermal and mechanical properties of chitosan and poly(vinyl alcohol) (PVA) with inter- and intra-hydrogen bonds were investigated systematically by using X-ray, DSC, positron annihilation and viscoelastic measurements. Based on their individual properties, the characteristics of the blend films were estimated in relation to their morphology and mechanical properties as a function of chitosan content. The characteristics of the blend films were also analyzed in terms of the deviation from a simple additive rule of chitosan and PVA content. These results suggested that the miscibility of chitosan and PVA could be ensured by entanglement of the amorphous chain segments of chitosan and PVA. Further detailed analysis revealed that the chitosan content on the film surface is higher than that of the admixture content of chitosan after elongation, although the chitosan and PVA chains were crystallized independently. The elongation could be achieved for the blend films whose PVA content was higher than 50% and the drawn blend films were transparent. Thus, it may be expected that sufficiently entangled meshes formed between chitosan and PVA amorphous chains within the film, the PVA content being higher than 50%, were maintained under the elongation process.

Keywords: blends; chitosan; elongation; poly(vinyl alcohol)

Introduction

Chitin and chitosan are natural polymers produced in the shells of crabs, shrimps and lobsters which have not been utilized effectively to date. Chitin ranks second to cellulose as the most plentiful organic compound on earth. It has been reported that $10^{10} \sim 10^{11}$ tons of these raw materials in the form of crab, shrimp or lobster shells are produced annually, the majority of which is disposed of as waste.[1,2] Consequently, chitosan prepared by chemical modification of chitin has been one of the most beneficial natural resources to pursue economical utilities by the recycling of the waste matter.

Manmade poly(vinyl alcohol) (PVA) films and fibers are polymer materials which are known to biodegrade when disposed outside. This is attributed to the hydrophilic property of PVA. In spite of a number of published papers on PVA, the thermal and mechanical properties remain an unresolved problem because of the difficulty in measuring the much smaller change in crystallinity with respect to temperature in comparison with poly-α-olefin polymers such as polyethylene and polypropylene.

To develop recyclable materials on the viewpoints of environmental protection and ecology, as discussed above, mechanical properties of chitosan and chitosan/PVA blend films and the fibers are very important

[1] Graduate School of Humanities and Sciences, Nara Women's University, Kitauoya-nishimachi, Nara 630-8263, Japan
E-mail: m-matsuo@cc.nara-wu.ac.jp
[2] Institute of Resource Recycling, Kinki University, Nara 631-8505, Japan
[3] Human Environmental Sciences, Faculty of Human Environmental Sciences, Mukogawa Women's University, Nishinomiya 663-8558, Japan

to expand the utilities as industrial materials. However, the maximum draw ratio of chitosan films was only two times under steam and the Young's modulus was ca. 6 GPa, which is slightly lower than that of common industrial materials such as nylon 6, poly(ethylene terephthalate) and polypropylene fibers. This is due to the poor molecular orientation caused by the low draw ratio (two times). To pursue the wider utilities of chitosan, the admixture of chitosan into PVA is carried out to promote an increase in the Young's modulus, since PVA is one of a number of degradable synthetic polymers with good drawability. Blends of chitosan and PVA with good miscibility have been reported to provide good mechanical properties,[3–7] drug release control,[8,9] and an approach for producing polymeric packaging films for specific purposes.[10]

In several papers,[11–14] however, the two polymers have been reported to be essentially immiscible. They reported the difficult compatibility by differential scanning calorimetry (DSC), scanning electron microscopy (SEM), Fourier transfer infrared spectrum (FTIR), electron-probe micro-analyzer etc. Among them, Koyano et al. pointed out that the chitosan content is dependent upon the position of the film and chitosan is concentrated on the air-surface side of the films. As other information, however, Arvanitoyannis et al. reported that the difficulty could be mitigated by adding sorbitol and sucrose as plasticizer.

In the present work, first of all, the individual thermal and mechanical properties of chitosan and PVA as-cast films were investigated for as-cast films containing water and perfectly dried films in relation to molecular mobility of PVA chains by using X-ray, DSC, positron annihilation and viscoelastic measurements. Based on the results, the detailed characteristics of the blends were analyzed as a function of chitosan content in terms of the individual properties of chitosan and PVA. Further analysis was done for chitosan content on the film surface of drawn films by electron spectroscopy for chemical analysis (ESCA) and water-contact angle experiments.

Experimental Part

Preparation Method of Films

Chitosan powder used in this research was furnished by Funakoshi Co. Ltd with 85% of deacetylation and viscosity of $5 \sim 20$ cp. First of all, 2 g chitosan was dispersed in 100 mℓ distilled water and stirred for 30 min. 1 mℓ acetic acid was added into the chitosan aqueous solution and mixed for 24 h at room temperature. The PVA powder of Nacalai Tesque. Inc. used as a sample had a degree of polymerization of 2000 and 98% hydrolysis. The PVA powders were dissolved in distilled water to maintain a 3% solution concentration and stirred for 40 min at 95 °C. After, the solution was cooled down to room temperature. The corresponding solution of chitosan and PVA, respectively, were simultaneously poured into a flask in the desired proportion of chitosan/PVA and stirred for 3–5 h at room temperature. The weight compositions chosen were 100/0 (chitosan homopolymer), 61/39, 50/50, 40/60, 30/70, 22/78 and 0/100 (PVA homopolymer). The mixed solution was poured into a petri-dish and the distilled water was allowed to evaporate to produce the cast film. The resulting film was first immersed into 4% sodium hydroxide for 2 h to neutralize the cast film, and then washed well with distilled water. Finally, the film was vacuum-dried for 1 day to remove residual traces of water and then placed inside a desiccator to avoid moisture absorption.

The resultant as-cast films were cut into strips, 60 mm long and 10 mm wide and then clamped in a manual stretching device in such a way that the length to be drawn was 40 mm. The specimens were placed in an oven at 160 °C and elongated manually a desired number of times after preheating for 5 min. The maximum draw ratios were 3 times ($\lambda = 3$) for the 40/60, 5 times ($\lambda = 5$) for the 30/70, 7 times ($\lambda = 7$) for the 22/78 and 8 times ($\lambda = 8$) for the 0/100. The

elongation was done smoothly without any partial breaking and the drawn blend films were transparent. Here, we must emphasize that the uniform mixing of the mixed solution (the chitosan content being higher than 50%) was very difficult and any elongation of the non-uniform resultant blend films was impossible.

Measurements of Characteristics of Chitosan, Chitosan/PVA Blend and PVA Films

The structures of the crystallites of chitosan, chitosan/PVA blend and PVA films were also estimated using a 12 kW rotating-anode X-ray generator (Rigaku RDA-rA) operated at 150 mA and 40 kV. The X-ray beam using CuKα radiation was monochromatized with a curved graphite monochromator. The diameter of the X-ray cell tube was 1 mm. WAXD intensity measurements were carried out using two methods. The first was a step-scanning method with a step interval of 0.1 ° taken at each fixed time of 40 sec, from 10 to 30° at a temperature of either 25 or 130 °C, and the second, a curved position-sensitive proportional counter (PSPC) to estimate the change in diffraction intensity distribution as a function of twice the Bragg angle simultaneously at a temperature ranging from −40 to 50 °C.

Positron annihilation experiments were conducted with a conventional fast-fast coincidence system having a time resolution of 300 ps full width at half-maximum (FWHM). The positron annihilation spectrometer was composed of two plastic scintillation detectors (40 mm diameter × 40 mm Pilot-U mounted on a Hamamatsu H1949 photomultiplier), two differential constant-fraction discriminators (ORTEC 583) (one for the start signals from 1.27 MeV γ-rays and the other for the stop signals from 0.511 MeV annihilation γ-rays), a time-to-amplitude converter (ORTEC 4570), and a multi-channel analyzer with a 1024 conversion gain (SEIKO 7800). A positron source was prepared by depositing ca. 1.1 MBq (30 μCi) of aqueous ^{22}NaCl on a Kapton foil of 7 μm thickness and 10 × 10 mm area. After drying, the foil was covered with a second foil of similar size, and the edges of the two foils glued together with epoxy resin. The source was further sealed in a 3 μm Mylar foil and then sandwiched by two identical samples for positron annihilation measurements. The spot diameter of the ^{22}Na source was ca. 2 mm. During the measurements the samples were kept in a vacuum cell in which the temperature was controlled. Spectra were recorded every hour, and about $1 \sim 2$ million events were stored in each spectrum. The detailed procedure has been described elsewhere.[15]

The densities of all the chitosan/PVA blend films were measured using a density gradient tube with *n*-heptane and carbon tetrachloride as the medium at 20 °C. Since the density of the blend film was dependent on there being no moisture within the film, great care was taken to remove the moisture. The samples were cut into fragments, washed by ultra-sonic treatment in ethanol and then dried in vacuum for 1 day prior to measuring the density. The densities of the undrawn and drawn (5 times) PVA films were 1.277 and 1.289, respectively, indicating a slight increase due to the oriented crystallization of PVA by elongation.

The thermal behavior of the film was estimated in terms of its melting endotherm as determined by differential scanning calorimetry (DSC). The DSC was performed using a DSC6200 (SII EXSTAR 6000) with 10 mg samples in standard aluminum pans. The samples were heated at a constant rate of 5 °C/min under nitrogen. The measurements were done in the temperature range from −130 to 400 °C.

The complex dynamic tensile moduli were measured at a frequency of 10 Hz over the temperature range from −150 to 300 °C by using a viscoelastic spectrometer (VES-R, Iwamoto Machine Co. Ltd.). The length of the specimen between the spectrometer jaws was 30 mm, and the width was ca. 5 mm. The measurements were described in detail elsewhere.[16,17]

The surface of the chitosan/PVA blend film was analyzed by electron spectroscopy for chemical analysis (ESCA-850, Shi-

madzu). The sample was irradiated with monochromated MgKα X-rays (8 kV, 30 mA) and the scanning speed was 0.05 V/s.[18] Water-contact angle experiments were performed using a Kyowa Interface Science Instrument, CA-X.

Results and Discussion

Figure 1 shows the densities of undrawn blend films with respect to chitosan content. The measured densities increased linearly with increasing chitosan content, indicating that the crystallization of PVA did not occur by admixing chitosan. To confirm this tendency, X-ray measurements were done at room and elevated temperatures.

Figure 2(a) and (b) show the X-ray diffraction intensity curves from chitosan, PVA and four chitosan/PVA blend films (61/39, 50/50, 40/60, 22/78) measured at 25 and 130 °C, respectively. The curves were drawn in the range of twice the Bragg angle from 16 to 24°. The open circles show the overlapped experimental intensity. Regarding the preliminary experiments, the temperature dependence of the X-ray intensity distribution was measured at 25, 60, 100, 140 and 180 °C for the undrawn chitosan and PVA films, in which the diffraction peaks associated with the chitosan and PVA crystallites appeared at the same diffraction angle independent of the measured temperature. This indicates that thermal crystallization does not occur for chitosan and PVA films due to molecular motion at elevated temperature, which is quite different from the thermal behaviors of certain poly-α-olefins such as polyethylene and polypropylene. Such poor chain mobility is thought to be due to the strong intra- and inter-hydrogen bonds between the PVA chains. The diffraction peaks from the (110), $(1\bar{1}0)$ and (200) planes of the PVA crystallites were overlapped because of low crystallinity. The diffraction peak associated with chitosan was also very weak indicating low crystallinity. The diffraction intensity profile of the chitosan and PVA crystallites within the blends also showed a very broad overlapped peak. According to Sakurai et al.,[19] the crystal units of chitosan were reported to be dependent upon the dissolved solvents used to prepare the films. The present chitosan film prepared from distilled water containing acetic acid provided a very broad peak profile.

The rough and fine dotted curves obtained by the peak separation shown in Figure 2 belong to the diffraction intensity distributions from the chitosan and PVA crystallites, respectively. The peak separation was done by assuming symmetrical profiles for each diffraction curve from chitosan and PVA crystallites. The fitting of

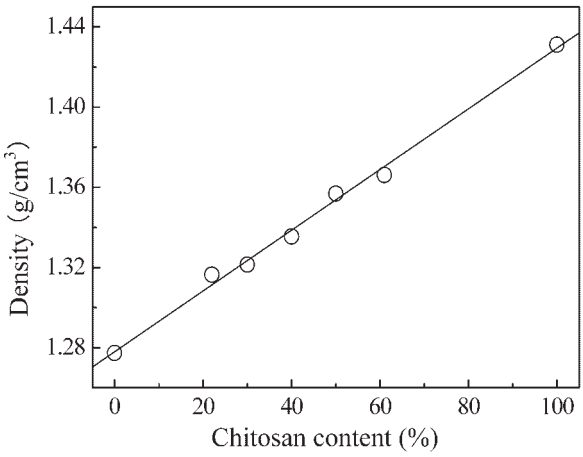

Figure 1.
Density of the undrawn blend films as a function of chitosan content.

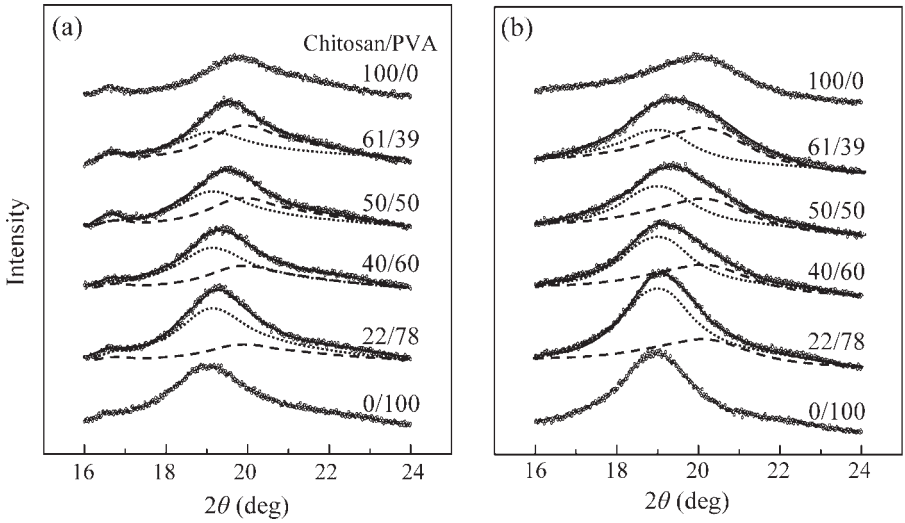

Figure 2.
WAXD intensity curves of chitosan (100/0), chitosan/PVA blend (61/39, 50/50, 40/60, 22/78) and PVA (0/100) films observed at (a) 25 °C and (b) 130 °C. ---- diffraction from chitosan, ... diffraction from PVA, — diffraction from the total.

the overlapped peak profiles observed for the chitosan and PVA crystallites within each blend film were initially given as a volume fraction ratio of chitosan/PVA calculated from the weight composition, and the volume fraction given as a parameter was slightly changed till the best fitting was achieved. The solid curve, which is the summation of the two separated curves, is in good agreement with the experimental results (open circles). The two separated curves for the four specimens at 25 and 130 °C showed the same profile indicating no thermal crystallization. The peaks appearing at 19.3° and 20.2° belong to the chitosan and PVA crystallites, respectively, and any observed peak shift did not occur as a result of changes in the chitosan/PVA compositions. This indicates that blending of chitosan and PVA had no effect on the crystallization of the two polymers. Namely, the observed result represented by open circles shows the simple overlapped peak from the individual chitosan and PVA crystallites. This means that the crystallization of chitosan and PVA occurred independently under evaporation of the solvent. Of course this estimation is only a qualitative analysis, since a detailed quantitative analysis was impossible for the very broad overlapped peak.

Thermal Properties of the Blend Film

Figure 3(a) shows the DSC curves of original as-cast chitosan, chitosan/PVA blend and PVA films measured in the temperature range from −130 to 250 °C. The DSC curve of the PVA film (0/100) shows an endotherm peak around 223 °C corresponding to the apparent melting point of the PVA crystallites, where the peak became smaller with decreasing PVA content. Here, it should be noted that the peak position (ca. 223 °C) shifted to higher temperature by admixing with chitosan and the shifted peak position (ca. 228 °C) was maintained at the same temperature independent of the chitosan content. Judging from the absence of the melting peak of chitosan, the peak shift for the blends is thought to be due to the appearance of the slightly modified PVA crystal unit by admixing with chitosan. This phenomenon must be carefully considered in relation to the miscibility of the chitosan and PVA chains, since a very small peak appeared at ca. 250 °C for the blend films, but did not appear for the chitosan and PVA films, as

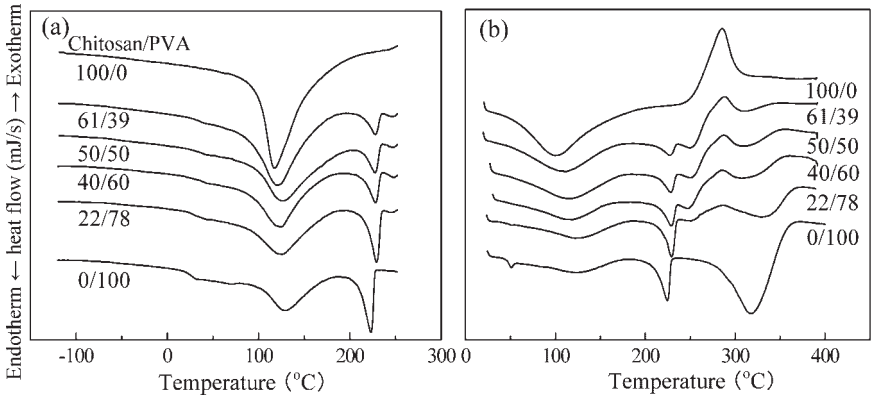

Figure 3.
DSC curves of chitosan (100/0), chitosan/PVA blend (61/39, 50/50, 40/60, 22/78) and PVA (0/100) films observed in the temperature range (a) from −130 to 250 °C and (b) from 25 to 400 °C.

shown in Figure 3(b). The appearance of the slightly modified PVA crystallites, however, remains an unresolved problem. In the established papers for chitosan and PVA blend films,[6,13,14] the main endothermic peak of PVA appearing at ca. 223 °C reported peak shift to lower temperatures. The appearance of the modified crystal, however, cannot be discussed with respect to the present specimens. Because the modified peak could not be confirmed by X-ray diffraction intensity curves showing the very broad overlapped peak of the chitosan and PVA crystallites (see Figure 2). Incidentally, we may emphasize that the large peak of the PVA film appearing at ca. 330 °C in Figure 3(b) is associated with the chain scission (depolymerization) and carbonization. Actually, it was confirmed that the black color film carbonized at 400 °C provided no peak under repeated heating process.

Here, it may be noted that the large broad peak of the chitosan film (100/0) formed at lower temperature (100 ∼ 150 °C) in Figure 3(a) becomes smaller and is shifted to higher temperature with increasing PVA content. Judging from the temperature dependence of the X-ray diffraction curves shown in Figure 2, it may be expected that this endothermic peak of each specimen is obviously independent of thermal crystallization and is related to the large movement of amorphous chains with pyranose rings. If this is the case, the broad peak shift to higher temperature with increasing PVA content is thought to be due to the comobility of chitosan and PVA amorphous chains associated with the miscibility of the two amorphous chain segments.

In spite of this active chain mobility, any thermal crystallization of the chitosan and PVA chains did not occur as shown in Figure 2. According to the established results by Chuang et al.[12] and Yang et al.[14], the appearance of a large broad peak at 110 ∼ 130 °C in Figure 3 was attributed to the influence of water molecules on the chain mobility. To check this, more detailed DSC measurements were carried out for the heating cycles.

Figure 4 shows DSC curves for chitosan (100/0), chitosan/PVA blend (22/78) and PVA (0/100) films, in which curves (a) and (b) in each column correspond to the first and second heating runs, respectively. The first heating run was conducted up to 160 °C lower than the endothermic peak (ca. 225 °C) to avoid chain scission (depolymerization) and carbonization, and then cooled to 25 °C. No exothermic peak was observed during the first cooling process. After heating above 250 °C during the second run, the exothermic peak for chitosan film disappeared, while peaks for PVA and the blend films appeared. The second heating

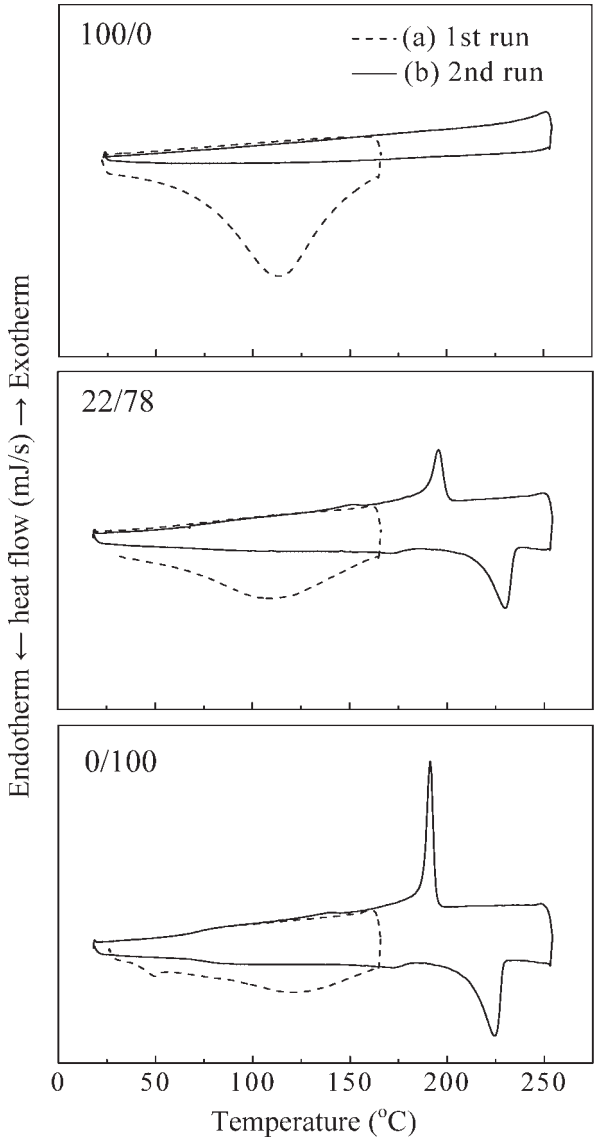

Figure 4.
DSC curves of chitosan (100/0), chitosan/PVA blend (22/78) and PVA (0/100) films measured under repeated heating and cooling processes: (a) the first heating from 25 to 160 °C and (b) the second heating from 25 to 250 °C.

run provided no broad endothermic peak at low temperature (120 °C). Accordingly, two possibilities to this phenomenon can be arisen. 1) The broad endothermic peak by the first heating run is related to the active mobility of the amorphous chain segments caused by the presence of small amounts of water molecules which play an important role as a plasticizer by disruption of the inter-chain hydrogen bonds between the chitosan chains, where most of the water molecules within the amorphous region were evaporated by the heating up to 160 °C. 2) The broad peak is only due to the evaporation of bounded water containing the specimens by the first heating up to

160 °C. Of course, the water evaporation was confirmed by TGA measurements, in which the weight loss occurred drastically during the first heating run up to 160 °C, and no change in weight loss was confirmed during the second heating because of the evaporation of the water molecules. The question shall be discussed later together with the results in Figure 7.

Figure 5 shows the DSC curves of the PVA film measured under the repeated heating and cooling processes from 25 to 250 °C after the first heating run up to 160 °C, as shown by the dotted line. The endothermic peak area became smaller and shifted to a lower temperature with an increasing number of heating cycles. Such thermal behavior is quite different from polymers such as polyethylene (PE) and polypropylene (PP) which have no hydrogen bonds. In spite of an increase in the number of repeated cycles, the DSC curves of PE and PP showed the same profile ensuring the reversibility of melting and crystallization. On the other hand, PVA with intra- and inter-hydrogen bonds underwent a chemical reaction at the apparent melting point around 225 °C, leading to chain scission and progression of carbonization causing a decrease in the number of PVA crystallites, as confirmed by the disappearance of the endothermic and exothermic peaks.

Figure 6(a) and (b) show the DSC curves for chitosan/PVA blend (40/60 and 22/78) and PVA (0/100) films itself in the undrawn and maximum drawn states, respectively. The curves for the undrawn films, which are shown in Figure 3, are shown again in Figure 6(a) to compare them with the thermal behavior concerning the apparent melting point of the drawn films. For each PVA content, the endothermic peak of the drawn film became noticeably sharper than that of the undrawn film, indicating an increase in the crystallinity of the PVA film due to the oriented crystallization, and this result was confirmed by the corresponding heat of fusion ΔH values listed in Figure 6. The increase in crystallinity by elongation is thought to be due to the fact that the amorphous PVA chains are oriented with respect to the stretching direction and the ordering of the amorphous chains became significant for oriented crystallization. Under the elongation process at 160 °C, it is evident that most of the water molecules between amorphous chains were extruded by promoting molecular ordering under oriented crystallization.

Interestingly, in Figure 6(b), the peak of the drawn 22/78 blend film ($\lambda = 7$) appeared at higher temperatures in comparison with the peak of the drawn PVA film ($\lambda = 8$) and this tendency is similar to that of the undrawn film as shown in Figure 6(a). As

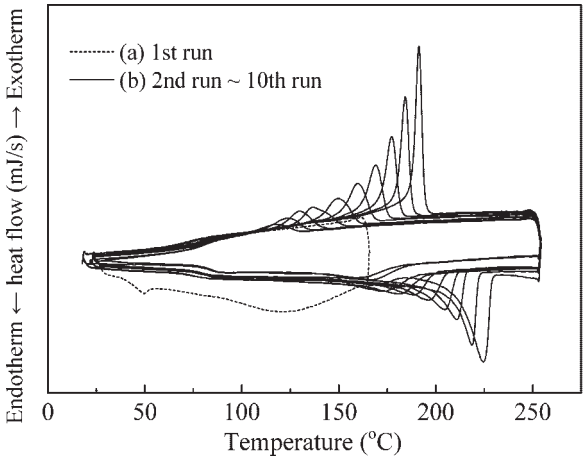

Figure 5.
DSC curves of PVA film (0/100) measured under repeated heating and cooling processes from 25 to 250 °C.

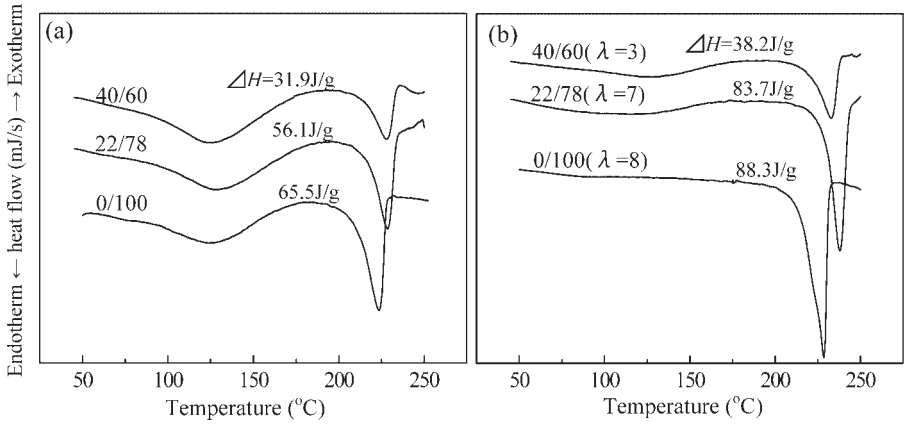

Figure 6.
DSC curves of PVA (0/100) and chitosan/PVA blend (40/60 and 22/78) films: (a) undrawn state, (b) drawn state.

can be seen in the curves of the 22/78 blend film with $\lambda = 7$, the apparent melting point appeared at ca. 238 °C higher than the peak (226 °C) of the PVA drawn film. This means that new crystallites associated with the miscibility of the chitosan and PVA chains become more stable as the draw ratio increases. However, we must emphasize again that any information to support the new crystallites could not be confirmed by X-ray measurements.

Mechanical Properties

Figure 7 shows the temperature dependence of the storage modulus (E') and loss modulus (E'') at a frequency of 10 Hz for chitosan (100/0), chitosan/PVA blend (40/60 and 22/78) and PVA (0/100) films. The results for the second heating run were shown as figures. The first heating run was performed from −150 to 160 °C, and the sample cooling was done from 160 °C to room temperature. After, each specimen

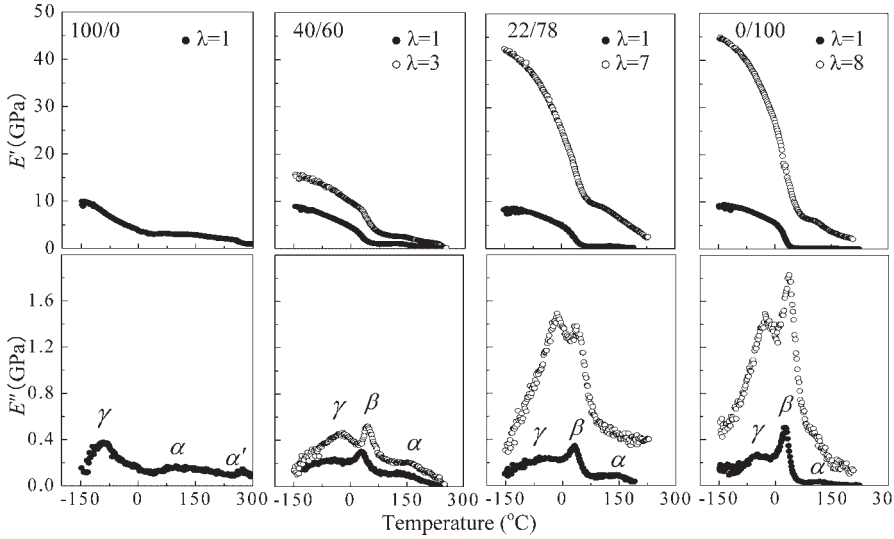

Figure 7.
Temperature dependence of the storage modulus (E') and the loss modulus (E'') at a frequency of 10 Hz for chitosan (100/0), chitosan/PVA blend (40/60 and 22/78) and PVA (0/100) films.

was cooled down to −150 °C in liquid nitrogen and then heated again up to 230 °C. Interestingly, the E' and E'' curves for the first heating run up to 160 °C almost overlapped with the curves for the second heating run, as shown in Figure 7, indicating that the E' and E'' of original as-cast chitosan, chitosan/PVA blend and PVA films vacuum-dried at room temperature are hardly affected by the mobility of the amorphous chain segments of chitosan and PVA due to the active mobility of water molecules detected clearly by the DSC measurements (see Figure 4). Namely, it is probably reasonable to consider that the temperature dependence of the E' and E'' are strongly dependent upon the intrinsic mechanical dispersions of the chitosan and PVA films, but the present condition, however, is different from the conditions[20–23] reported for the chitosan films containing moisture. Accordingly, the broad peak shown in Figure 4 is probably thought to be due to only evaporation of bounded water connected tightly with hydrogen groups of amorphous chain segments of chitosan and PVA chains.

A detailed observation reveals that the decrease in E' for the chitosan film tended to level off in the temperature range 0 ~ 50 °C, although E' for the PVA and blend films decreased with increasing temperature. The E'' curve of the chitosan film exhibits three peaks. The first peak appearing around −100 °C is termed the γ dispersion peak, while the second peak around 120 °C is termed the α dispersion peak. The third peak termed as the α' dispersion peak appeared at ca. 275 °C. The γ dispersion peak is thought to be due to the motions of different groups with different steric or energetic interactions. The hindered rotation of the pyranose rings around the ether bond below the glass transition temperature provides one of the possibilities. The second (α) dispersion peak is very broad. Judging from the DSC results discussed already, the α dispersion is obviously not attributed to the crystalline region, but to the amorphous region. According to the results of Sakurai et al.[20] for the chitosan film, the peak represented as tan δ appeared around 155 °C under the first heating process, and the peak appeared as a shoulder in the range from 200 to 210 °C under the second heating run. Furthermore, Sakurai et al.[20] pointed out that the glass transition temperature of the chitosan film is 203 °C by DSC measurements. Further experiments for chitosan were reported by Pizzoli et al.,[21] Ogura et al.[22] and Miyashita et al.[23] Most of their discussions[21–23] were focused on the mechanical properties and glass temperature of the chitosan films in both wet and dry states, and these authors reported that the glass temperature of chitosan is ca. 200 °C, while the E' and E'' values are sensitive to the moisture in the film.

In the present work, the endothermic peak of chitosan in Figure 3 and 4 is related to the α dispersion peak of E'' in Figure 7, indicating that the α dispersion is attributed to the active mobility of the amorphous chains. Accordingly, the active amorphous chain mobility associated with the α dispersion is thought to be due to the disruption of the inter-chain hydrogen bonds by the active mobility of the water molecules remaining between the chitosan chains in spite of the first heating run up to 160 °C. Furthermore, the peak appearing at ca. 275 °C, termed as the α' dispersion peak, may be associated with crystal dispersion, which is thought to be in good connection with the exothermic peak of the chitosan film (100/0) at ca. 285 °C in Figure 3(b).

In contrast, for the undrawn PVA film, there were three different peaks from the high temperature side termed the α, β and γ dispersion peaks. The E' value of the PVA film decreased drastically in the temperature range from 5 to 50 °C. This temperature range is much lower than the endothermic peak of the PVA film (see Figure 3(a)). The analysis of this peak shall be discussed in relation to the positron annihilation results later.

It is seen that E'' for undrawn PVA film shows broad and sharp peaks around −35 and 30 °C, respectively, which are termed as the γ and β peaks, respectively. Similar

peaks appearing below 0 °C were observed by Nishio et al.,[24] and in their study, other peaks located at about 80 and 35 °C were reported as the dispersions due to relaxations in the amorphous PVA regions, and the dispersions observed above 100 °C were due to the crystalline relaxations of PVA.

As for the drawn films, E' of the 22/78 ($\lambda = 7$) and the 0/100 ($\lambda = 8$) decreased drastically with increasing temperature up to 50 °C. E'' provided a large peak at around 30 °C, indicating that E' and E'' are strongly affected by the macro-Brownian movement of amorphous chain segments of PVA associated with the β dispersion. Certainly, at the frozen state of the macro-Brownian movement, the preferential orientation of crystal and amorphous chains with respect to the stretching direction offered high storage modulus. But it may be expected that the oriented amorphous chains are isolated independently and do not form the aggregation similar to para-crystallites with inter-chain hydrogen bonds between PVA chains.

In accordance with the undrawn PVA film prepared from a (70/30) mixture of dimethyl sulfoxide (Me_2SO) and water, the corresponding γ and β peaks appeared at -70 and -10 °C, respectively, and the peaks were much broader.[25] This indicates that the fluctuation in the chain arrangements in the amorphous phase for the PVA film prepared from aqueous solution is larger than that for the PVA film prepared from a Me_2SO/water mixture.

Further analysis of the chitosan/PVA blend film was done in terms of the simple additivity of the complex moduli of chitosan and PVA. Theoretical calculations were carried out as a function of chitosan content by using the three-dimensional model in Figure 8,[26–28] in which the chitosan layers are surrounded by a PVA plane, so that the strains of the two phases at the boundary in three directions are identical. The parameters δ, υ and μ correspond to the fraction length of chitosan in the three directions, and the volume fraction of chitosan is given as $\delta\upsilon\mu$. By using the model system, the complex

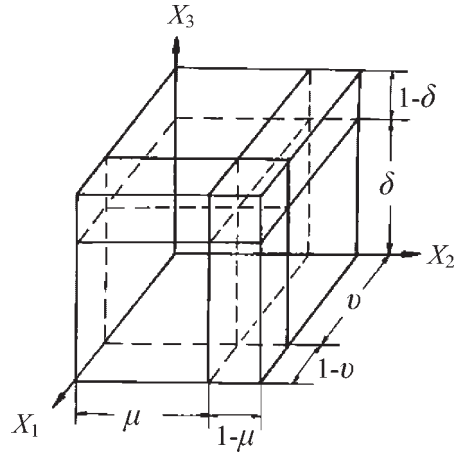

Figure 8.
A composite model in which the oriented crystallites are surrounded by an anisotropic amorphous phase.

moduli of the blend may be given by:

$$E^* = \frac{E_2^*\{E_1^*(1-\delta)+\delta E_2^*(1-\upsilon\mu)+\delta\upsilon\mu E_1^*\}}{E_1^*(1-\delta)+\delta E_2^*} \quad (1)$$

In Equation (1), E_1^* and E_2^* are the complex moduli of chitosan and PVA films in the non-deformed state. The derivation of Equation (1) is given in Appendix.

The values of the three parameter δ, υ and μ are unknown factors, while the volume fraction $\delta\upsilon\mu$ is known. It is generally reasonable to assume that $\delta = \upsilon = \mu$ for an undrawn film.[26–28] In this case, Equation (1) may be rewritten as:

$$E^* = \frac{E_2^*\{E_1^*(1-\delta)+\delta E_2^*(1-\delta^2)+\delta^3 E_1^*\}}{E_1^*(1-\delta)+\delta E_2^*} \quad (2)$$

As shown in Figure 9, the theoretical solid curves are in good agreement with the experimental results indicating that the two complex moduli of chitosan and PVA satisfy the simple additivity of Equation (2). This suggests that the crystallization of the PVA chains is almost independent of the chitosan content, and this concept also supports the linear relationship for the density of the blend film with respect to the chitosan content, as shown in Figure 1.

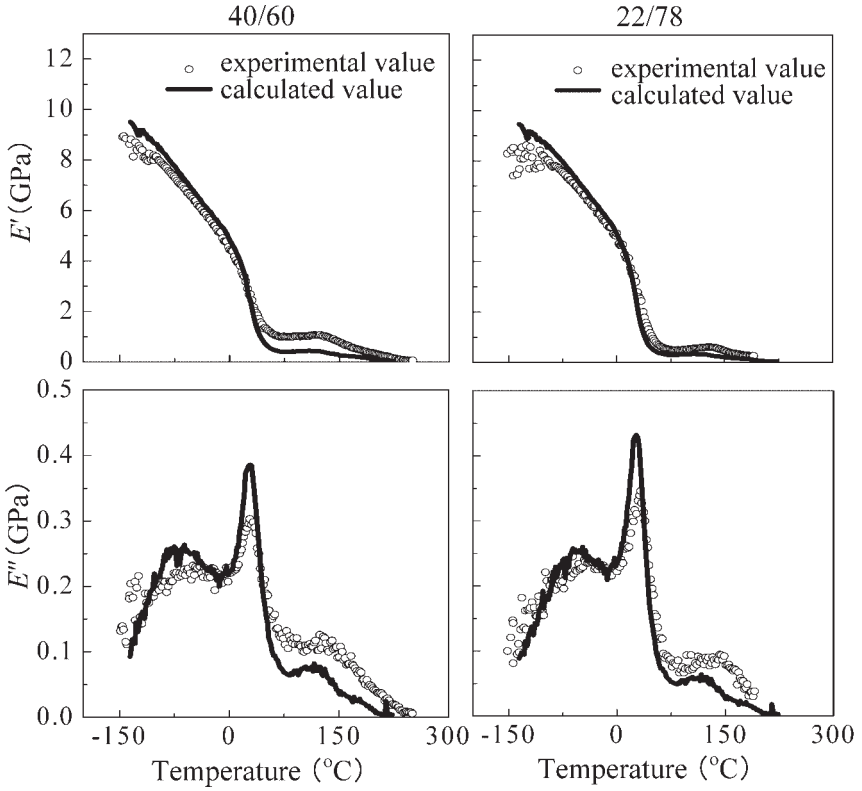

Figure 9.
The theoretical and experimental results of the storage modulus (E') and the loss modulus (E'') at a frequency of 10 Hz for chitosan/PVA blend films (40/60 and 22/78).

Figure 10 shows no change in the X-ray diffraction peaks observed for chitosan, chitosan/PVA blend (22/78) and PVA films in the temperature range from −40 to 50 °C, indicating that the β dispersion peak of E'' around 30 °C in Figure 7 is independent of thermal crystallization. Accordingly, the β dispersion peak is related to the active mobility of the PVA amorphous chains associated with macro-Brownian motion and this concept supports the drastic decrease of the corresponding E'.

An increase in the average free volume holes can be clearly monitored by positron annihilation. Positron annihilation is one of the useful techniques to investigate relaxation characteristics of polymers. Positrons emitted from ^{22}Na induce radiation effect on polymer samples, and then resultant electrons are trapped in a shallow potential, which are formed at low temperature far below the glass temperature (Tg). The increase in the number of these trapped electrons is observed as an increase in the intensity (I3) of the long-lived component of ortho-positronium (o-Ps).

Figure 11(a) and (b) shows temperature dependence of the intensity (I_3) and the lifetime (τ_3), respectively, of the long-lived component due to *o-Ps* pick-off annihilation[29–33] are given as a function of the temperature for the PVA film. The heating rate was 5 °C/h. I_3 is the quantity of the *o*-Ps formation probability. Although τ_3 has been successfully correlated to the average size of the free volume holes present in polymers, I_3 has been found to be influenced by many factors, such as the temperature, positron irradiation, electric field and polar group.

With increasing temperature, τ_3 increases as shown in Figure 11(a). In this figure, there

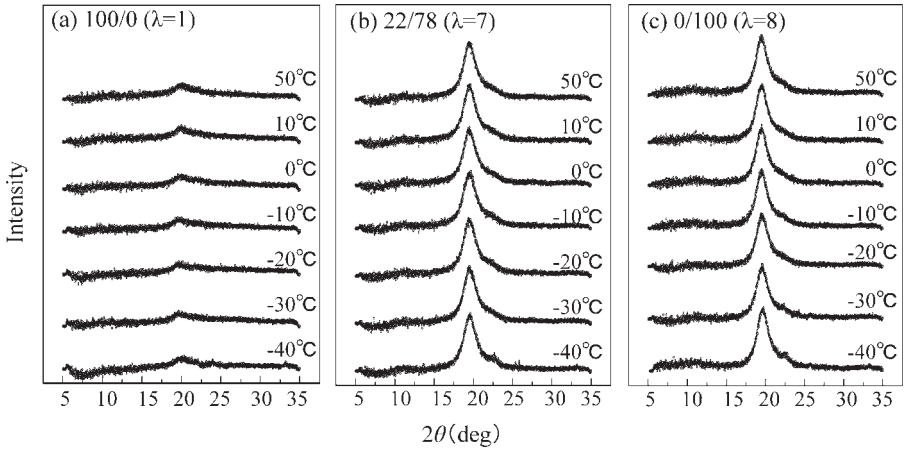

Figure 10.
WAXD intensity measured in the temperature range from −40 to 50 °C: (a) chitosan film (100/0), (b) chitosan/PVA blend film (22/78) with $\lambda = 7$ and (c) PVA film (0/100) with $\lambda = 8$.

is one transition at ca. −30 °C. The transition appeared at the same temperature as that for the γ dispersion peak, as shown in Figure 7. According to the correlation between τ_3 and the free volume size,[29] the γ-dispersion has been explained as being the contribution from the glass transition associated with the free volume due to localized motion of the local group of amorphous chains. If this is the case, the glass transition temperature (*Tg*) of PVA must be −35 °C corresponding to the γ dispersion.

Tg of PVA was reported to be around 85 °C by Masci et al.,[34] on the basis of the appearance of the very broad peak, and in agreement with the value reported elsewhere.[35] On the other hand, Yang et al.[14] estimated that *Tg* is ca. 71 °C corresponding to a sudden change of DSC curve. Although 70 ∼ 85 °C is certainly the well-established value of *Tg,* the first transition of τ_3 suggests that *Tg* of PVA is around −30 °C, which is in good agreement of a decrease of E' with temperature. If the glass transition temperature must be defined as the starting point of the drastic decrease in Young's/shear modulus, it must reflect the γ dispersion. Actually, it was confirmed that the first transition by positron annihilation

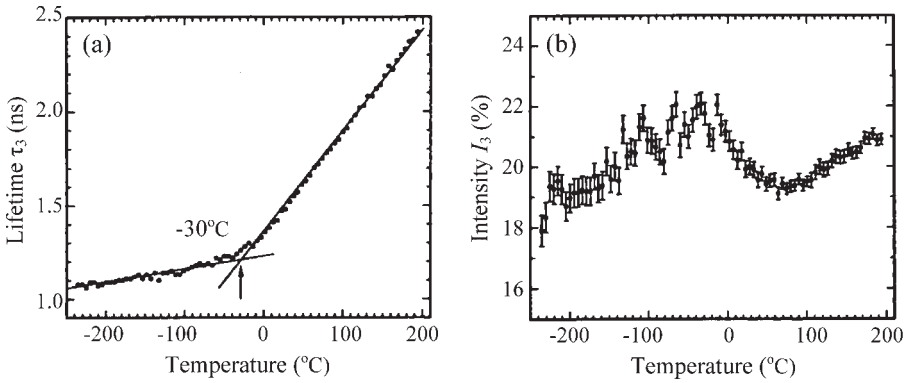

Figure 11.
Temperature dependence of the corresponding lifetime (τ_3) and the intensity (I_3) for the long-lived component due to o-Ps pick-off annihilation of PVA film (0/100).

corresponded to the γ dispersion for several kinds of polyethylene films and the glass transition was related to the γ dispersion.[17,36] Unfortunately, the glass transition temperature of the chitosan film could not be discussed on the basis of the first transition of τ_3, since the values of τ_3 and I_3 were scattered.

As can be seen in Figure 11(b), the temperature dependence of I_3 for PVA is similar to that of polyethylene.[36] It can be seen that I_3 increases as a function of temperature up to $-10\,^{\circ}C$. The increase in I_3 has been proved to be due to the positron irradiation effect on a polymer at low temperature. The secondary electrons that escape from the positron spur could be easily trapped in shallow potentials formed between the polymer chains when the motions of the molecular chains and groups are frozen at low temperature. Due to the positron irradiation time (experimental time), the probability of *Ps* formation would become larger. As can be seen in this figure, I_3 becomes a maximum at around $-10\,^{\circ}C$, and begins to decrease with increasing temperature. I_3 attains a minimum at ca. $75\,^{\circ}C$ and increases again beyond ca. $75\,^{\circ}C$. This is due to an apparent increase in the number of holes detected by positron annihilation, because of the thermal expansion of the holes at elevated temperature. The very small holes, which could not be detected by positron annihilation at temperatures $<75\,^{\circ}C$, can be detected by an increase in their size as a result of thermal expansion.

In accordance with Suzuki et al.,[37] the minimum temperature of I_3 is due to the fact that the local motion causes a large (macro-Brownian) correlated movement of the polymer chains in the amorphous phase. Accordingly, the movement may erase most of the shallow potentials; the trapped electrons may then also disappear. If this is the case, the molecular motion at low temperatures affects the concentration of trapped electrons in a shallow potential, and consequently, the variation in I_3 is closely related to the relaxation temperature as a second effect. In this experiment, it turns out that the β dispersion associated with the large movement of amorphous chains approximately corresponds to the minimum region ($75\,^{\circ}C$) of I_3, although the dispersion peak of E'' appeared around $30\,^{\circ}C$ (see Figure 7). Interestingly, $75\,^{\circ}C$ corresponding to the Tg ($70 \sim 85\,^{\circ}C$) value of PVA reported elsewhere.[14,34] This indicates that the established value of Tg is related to the local motion of large (macro-Brownian) movement. However, further consideration must be taken into account to lead to more conclusive evidence.

Surface Properties of the Blends

To study the surface characteristics, the peak separation attributed to the carbon atoms as confirmed by ESCA measurements was carried out for chitosan (100/0), chitosan/PVA blend (40/60 and 22/78) and PVA (0/100) films, the results of which are shown in Figure 12. Of course, the correction of the photo-ionization cross section was done. The peak separation was performed by the established method reported for C–C and C–H (peak 1), C–O (peak 2), C–NH (peak 3) and O–C=O (peak 4).[38–41] The total curve (dotted curve) corresponding to the summation of each peak magnitude gave the best fit with respect to the measured curve (solid curve). The peak area fractions of the specimens are listed in Table 1. Peak 3 associated with chitosan became more intense with increasing draw ratio. This reveals that the chitosan content on the surface of the blend films increases with increasing draw ratio.

Figure 13 shows the N_{1s}/C_{1s} ratio with respect to the chitosan content for the undrawn blend films, and the draw ratio for chitosan (100/0) and chitosan/PVA blend (40/60 and 22/78) films, in which the N_{1s}/C_{1s} ratio corresponds to the normalized value of the N_{1s} peak area by C_{1s} peak area given as a summation of four components in Figure 12. As shown in Figure 13(a), the component of the N_{1s} peak area associated with the content of chitosan is much smaller than that of the C_{1s} peak area. However, the increasing tendency of the N_{1s}/C_{1s} ratio

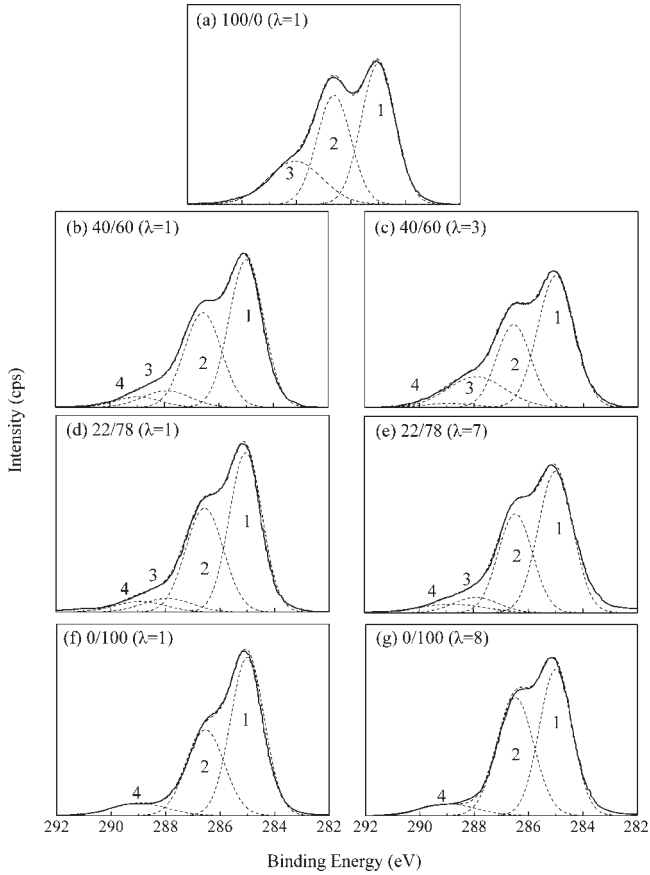

Figure 12.
C_{1s} spectra afforded by ESCA measurements of (a) the undrawn chitosan film (100/0), (b)–(e) the undrawn and drawn chitosan/PVA blend films (40/60 and 22/78) and (f)(g) the undrawn and drawn PVA films (0/100).

with respect to the draw ratio can be recognized. If the dispersion of chitosan is uniform within the blend film, the value must be independent of draw ratio. The increasing tendency is significant for the 40/60 blend, indicating that the chitosan content on the blend film surface increases with increasing draw ratio. This is probably thought to be due to the fact that the surface energy of chitosan is lower than that of PVA.

Table 1.
The peak area of C_{1s} components by ESCA measurements.

	Peak No.	Peak area ratio (%)							
		1 (C–C,C–H)		2 (C–O)		3 (C–NH)		4 (O–C=O)	
chitosan	($\lambda = 1$)	44.38		34.11		21.51		–	
40/60	($\lambda = 1$)	51.64		35.80		7.92		4.64	
	($\lambda = 3$)		50.65		29.55		17.87		1.93
22/78	($\lambda = 1$)	54.27		34.25		6.38		5.10	
	($\lambda = 7$)		51.25		35.62		7.22		5.90
PVA	($\lambda = 1$)	57.77		34.95		–		7.28	
	($\lambda = 8$)		49.06		44.43		–		6.51

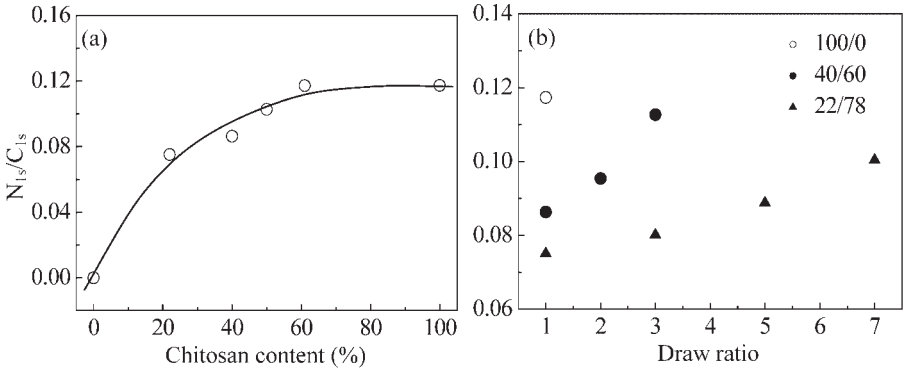

Figure 13.
The N_{1s}/C_{1s} ratio afforded by ESCA measurements with respect to (a) chitosan content for the undrawn films and (b) draw ratio for chitosan/PVA blend films (40/60 and 22/78) in addition to undrawn chitosan film (100/0).

Figure 14(a) and (b) show the corresponding changes in contact angle with respect to the chitosan content and the draw ratio, respectively, for the indicated blend films. The wettability of the chitosan film is confirmed to be less than that of PVA, and then the contact angle increases with increasing chitosan content. The contact angle for the PVA film decreases with increasing draw ratio, since the fraction of C–O increases, as listed in Table 1. The decrease in contact angle becomes less pronounced with increasing chitosan content at each draw ratio. This phenomenon is obviously reasonable, since the ESCA results revealed decreases in the number of C–O and O–C=O groups on the surface. The increase in chitosan content shown in Figure 12 and 13 together indicates that the surface of the drawn blend film must be compounded with chitosan chains and amorphous PVA chains. Such a sufficient number of entanglement meshes between the amorphous chitosan and PVA chains relates to good miscibility, and is very important to ensure uniform elongation of the blend films. Actually, no macrocracking was found to occur under the elongation process, and the drawn blend film was transparent.

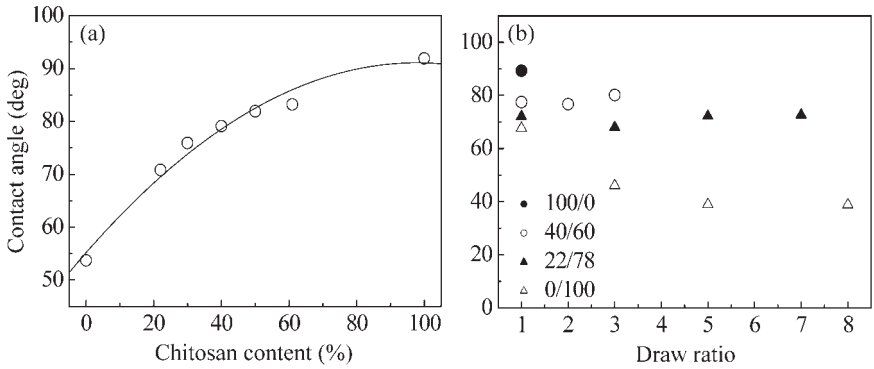

Figure 14.
The change in contact angle with respect to (a) the chitosan content for the undrawn films and (b) the draw ratio for the blend films (40/60 and 22/78).

The similar tendency was confirmed for the blends of ultra-high molecular weight polyethylene (UHMWPE) and ultra-high molecular weight polypropylene (UHMWPP) prepared by gelation/crystallization method.[42,43] The blend films provided intrinsic diffractions from the crystal planes of UHMWPE and UHMWPP indicating the separate crystallization of each chain. But the blend films could be elongated more than 80 times. Such high elongation is thought to be due to the entanglement meshes of UHMWPE and UHMWPP amorphous chains.

Conclusion

The morphology and physical properties of chitosan, chitosan/PVA blend and PVA films prepared from aqueous solution were investigated. The origins of the thermal and mechanical properties of chitosan and PVA with inter- and intra-hydrogen bonds were investigated systematically by using positron annihilation, DSC, X-ray and viscoelastic measurements. The broad endothermic peak appeared at $110 \sim 130\,^{\circ}C$ by the first heating up to $160\,^{\circ}C$ was associated with the evaporation of water containing the films and was hardly affected by the mobility of the amorphous chain segments of chitosan and PVA, since the E' and E'' curves for the first heating almost overlapped with the curves for the second heating run.. The transition of τ_3 by positron annihilation for PVA was related to the micro-Brawnian motion, while the decrease of I_3 is related to macro-Brawnian motion. Namely, the transition of τ_3 and the decrease of I_3 were in good relationship with γ and β mechanical relaxations of the amorphous phase, respectively. The physical properties of the undrawn chitosan/PVA blend films provided simple additivity given as a function of chitosan content, indicating the individual crystallization of chitosan and PVA. Even so, the endothermic peak of the DSC curve resulting from admixing with chitosan slightly shifted to higher temperature, indicating co-crystallization leading to good miscibility. A detailed analysis afforded by contact angle and ESCA studies indicated that the chitosan content on the blend polymer surface increased with increasing draw ratio. Accordingly, it may be expected that the entanglement meshes between the chitosan and PVA amorphous chains on the surface assured uniform elongation without any macro-cracking.

Appendix

In the model in Figure 8, the chitosan layers are adjacent to the PVA layers with the interfaces perpendicular to the X_1, X_2 and X_3 axes fixed within the bulk specimen. The strains of the two phases at the boundary are assumed to be identical. The model is constructed from three composites, as shown in Figure 15. In model (a), the PVA layer (A) with fraction length 1-δ lies adjacent to the chitosan layer (C) with the interface perpendicular to the X_3 axis, and in model (b) the PVA layer with fraction length 1-υ is attached to the structure of phase I in a plane normal to X_1 the direction. The final phase III can be constructed by adding a 1-μ PVA layer with fraction length to phase II. Accordingly, the complex moduli E_I^* of phase I is given from the viewpoint of a series model.

$$E_I^* = \frac{\delta}{E_1^*} + \frac{1-\delta}{E_2^*} \tag{A-1}$$

By using a concept of the parallel model, the modulus E_{II}^* of phase II and E_{III}^* (E^*) of phase III may be given, respectively, as:

$$E_{II}^* = \upsilon E_I^* + (1-\upsilon)E_2^* \tag{A-2}$$

and

$$E_{III}^* = \upsilon E_{II}^* + (1-\mu)E_2^* = E^* \tag{A-3}$$

Substituting Equation (A-1) and (A-2) into (A-3), Equation (1) may be obtained.

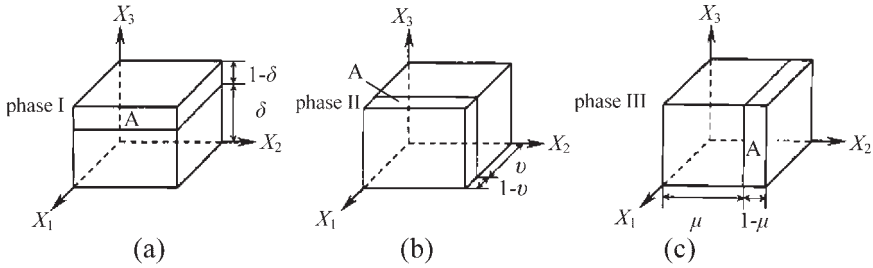

Figure 15.
A composite procedure for the construction of a model in Figure 8: (a) amorphous phase attached to the X_3 face of the crystallite to construct phase I, (b) amorphous phase attached to the X_1 face of phase I to construct phase II, (c) amorphous phase attached to the X_2 face of phase II to construct phase III.

Acknowledgements: The authors acknowledge the valuable discussion on positron annihilation with Prof. Takenori Suzuki from the Radiation Science Center of the High Energy Accelerator Research Organization.

[1] Y. Doi, Ed., "*Degradable Plastic*" (in Japanese), CMC Publishing Co., Ltd., Tokyo **1990**, p. 1–2, 107–117.
[2] Y. Doi, Ed., "*Polymeric Material of Biodegradability*" (in Japanese), Industrial Investigation Committee Kogyo Chousakai, Publishing Inc., Tokyo **1990**, p. 177–197.
[3] C. Castro, L. Gargallo, A. Leiva, D. Radic, *J. Appl. Polym. Sci.* **2005**, *97*, 1953.
[4] M. Miya, S. Yoshikawa, R. Iwamoto, S. Mima, *Kobunshi Ronbunshu* **1983**, *40*, 645.
[5] Y. Miyashita, Y. Nishio, T. Akamatsu, N. Kimura, H. Suzuki, *Sen-i Gakkaishi* **1999**, *55*, 254.
[6] Q. Wang, Y. M. Du, L. H. Fan, *J. Appl. Polym. Sci.* **2005**, *96*, 808.
[7] H. Zheng, Y. Du, J. Yu, R. Huang, L. Zhang, *J. Appl. Polym. Sci.* **2001**, *80*, 2558.
[8] C. G. L. Khoo, S. Frantzich, A. Rosinski, M. Sjöström, J. Hoogstraate, *Eur. J. Pharm. Biopharm.* **2003**, *55*, 47.
[9] J. H. Kim, J. Y. Kim, T. H. Lee, K. Y. Kim, *J. Appl. Polym. Sci.* **1992**, *45*, 1711.
[10] P. C. Srinivase, M. N. Ramesh, K. R. Kumar, R. N. Tharanathan, *Carbohydr. Polym.* **2003**, *53*, 431.
[11] I. Arvanitoyannis, I. Kolokuris, A. Nakayama, N. Yamamoto, S. Aiba, *Carbohydr. Polym.* **1997**, *34*, 9.
[12] W. Y. Chuang, T. H. Young, C. H. Yao, W. Y. Chiu, *Biomaterials* **1999**, *20*, 1479.
[13] T. Koyano, N. Koshizaki, H. Umehara, M. Nagura, N. Minoura, *Polymer* **2000**, *41*, 4461.
[14] J. M. Yang, W. Y. Su, T. L. Leu, M. C. Yang, *J. Memb. Sci.* **2004**, *236*, 39.
[15] L. Ma, C. He, T. Suzuki, M. Azuma, Y. Bin, H. Kurosu, M. Matsuo, *Macromolecules* **2003**, *36*, 8056.
[16] M. Matsuo, C. Sawatari, T. Ohhata, *Macromolecules* **1988**, *21*, 1317.
[17] M. Matsuo, Y. Bin, C. Xu, L. Ma, T. Nakaoki, T. Suzuki, *Polymer* **2003**, *44*, 4325.
[18] T. Okuno, Y. Nakano, K. Yoshida, K. Yokoyama, M. Hamaguchi, M. Matsuo, *Polym. J.* **2005**, *37*, 169.
[19] K. Sakurai, M. Takagi, T. Takahashi, *Sen-i Gakkaishi* **1984**, *40*, 114.
[20] K. Sakurai, T. Maegawa, T. Takahashi, *Polymer* **2000**, *41*, 7051.
[21] M. Pizzoli, G. Ceccorulli, M. Scandola, *Carbohydr. Res.* **1991**, *222*, 205.
[22] K. Ogura, T. Kanamoto, M. Itoh, H. Miyashiro, *Polym. Bull.* **1980**, *2*, 301.
[23] Y. Miyashita, Y. Yamada, N. Kimura, Y. Nishio, H. Suzuki, *Sen-i Gakkaishi* **1995**, *51*, 396.
[24] Y. Nishio, R. St, J. Manley, *Macromolecules* **1988**, *21*, 1270.
[25] Y. Bin, Y. Tanabe, C. Nakabayashi, H. Kurosu, M. Matsuo, *Polymer* **2001**, *42*, 1183.
[26] M. Matsuo, *J. Chem. Phys.* **1980**, *72*, 899.
[27] M. Matsuo, C. Sawatari, Y. Iwai, F. Ozaki, *Macromolecules* **1990**, *23*, 3266.
[28] M. Matsuo, Y. Bin, M. Nakano, *Polymer* **2001**, *42*, 4687.
[29] S. J. Tao, *J. Phys. Chem.* **1972**, *56*, 5499.
[30] T. Suzuki, Y. Oki, M. Numajiri, T. Miura, K. Konda, Y. Ito, *Radiat. Phys. Chem.* **1995**, *45*, 675.
[31] B. Levey, M. Lavoric, H. J. Ache, *J. Chem. Phys.* **1989**, *90*, 3282.
[32] Z. Zhang, Y. Ito, *Radiat. Phys. Chem.* **1991**, *38*, 221.
[33] J. Cerna, J. C. Abbe, G. Duplatre, *Phys. Status Solidi* **1989**, *A115*, 389.
[34] G. Masci, I. Husu, S. Murtas, A. Piozzi, V. Crescenzi, *Macromol. Biosci.* **2003**, *3*, 455.
[35] I. Sakurada, "*Polyvinyl alcohol fibers*", Marcel Dekker, New York **1985**.
[36] M. Matsuo, L. Ma, M. Azuma, C. He, T. Suzuki, *Macromolecules* **2002**, *35*, 3059.
[37] T. Suzuki, K. Kondo, E. Hamada, Y. Ito, *Radiat. Phys. Chem.* **2000**, *58*, 485.

[38] D. Anderson, T. Nguyen, P. N. Lai, M. Amiji, *J. Appl. Polym. Sci.* **2001**, *80*, 1274.
[39] L. Sigurdson, D. E. Carney, Y. Hou, L. Hall, III, R. Hard, W. Hichs, Jr., F. V. Bright, J. A. Gardella, Jr. *J. Biomed. Mater. Res.* **2002**, *59*, 357.
[40] Z. Ma, C. Gao, Y. Gong, J. Ji, J. Shen, *J. Biomed. Mater. Res.* **2002**, *63*, 838.
[41] B. Sreedhar, D. K. Chattopadhyay, M. S. H. Karunakar, A. R. K. Sastry, *J. Appl. Polym. Sci.* **2006**, *101*, 25.
[42] C. Sawatari, S. Shimogiri, M. Matsuo, *Macromolecules* **1987**, *20*, 1033.
[43] C. Sawatari, S. Satoh, M. Matsuo, *Polymer* **1990**, *32*, 1456.

